ROYAL SOCIETY
OF CHEMISTRY

PAPER

Check for updates

Facile preparation of antibacterial hydrogel with multi-functions based on carboxymethyl chitosan and oligomeric procyanidin†

Yuanmeng He, Shen Guo, Rong Chang, Dan Zhang, Yikun Ren, Fangxia Guan*
and Minghao Yao [ID] *

Hydrogel-based antibacterial materials with multi-functions are of great significance for healthcare. Herein, a facile and one-step method was developed to fabricate an injectable hydrogel (named CMCS/OPC hydrogel) based on carboxymethyl chitosan (CMCS) and oligomeric procyanidin (OPC). In this hydrogel system, OPC serves as the dynamic crosslinker to bridge CMCS macromolecules mainly through dynamical hydrogen bonds, which endows this hydrogel with excellent injectable, self-healing, and adhesive abilities. In addition, due to the inherent antibacterial properties of CMCS and OPC, this hydrogel shows excellent antibacterial activity. Therefore, the well-designed CMCS/OPC hydrogel has great prospects as an antibacterial material in the biomedical field.

1. Introduction

A hydrogel is a water-soluble polymer material with a unique three-dimensional (3D) structure.[1,2] Due to their high similarity to biological tissues and extracellular matrix (ECM), especially the water-rich, soft, and highly porous structure, hydrogels have been widely used in biomedical sensors,[3,4] cosmetics,[5] materials science,[6] tissue engineering[7] and other fields.

Adhesive hydrogels can be seamlessly attached to the desired sites for a long period of time, avoiding the potential risk of microbial infection, facilitating gas exchange, as well as avoiding the shedding of hydrogel due to frequent activity.[8,9] At present, *in situ* forming hydrogel has attracted more and more attention because of its unique injectable ability. The appeal of this approach is that injectable hydrogels can fill irregular structures perfectly.[10–12] Self-healing usually refers to the ability of a material to heal itself or repair fractures and defects and restore its structure and function after damage.[13,14] In recent years, hydrogels with self-healing ability have attracted great attention. Benefitting from their self-healing ability, hydrogels can have a much longer life as well as improved reliability and durability. In addition, due to the abuse of antibiotics, the emergence of drug-resistant bacteria makes the problem of bacterial infection more and more serious. It is estimated that more than 10 million people will die each year from antibiotic-resistant pathogens by 2050, therefore developing a better antibacterial strategy has become a topic of concern.[15,16]

Chitosan is a natural amino polysaccharide with poly-positive charge derived from shrimp and crab shells. Carboxymethyl chitosan (CMCS) is one of the derivatives of chitosan, which has better biocompatibility and solubility.[17–19] CMCS-based hydrogels are some of the most ideal candidates in biomedical fields such as tissue engineering, drug delivery systems and artificial skin due to their three-dimensional network, hydrophilicity and desired functionality.[20–25] Naturally derived polyphenols such as tannic acid, procyanidins, and dopamine have been found to possess antioxidant, antibacterial, and anti-inflammatory effects.[26–30] Inspired by the super adhesion of marine mussels in the humid environment, the underwater wet adhesion theory based on dopamine is widely known, and numerous dopamine-based and tissue-adhesive hydrogels have been developed.[28,31,32] Guo *et al.*, for example, reported a gelatin-grafted dopamine-based carbon nanotubes supported hydrogel with adhesive, injectable, antibacterial and other functions.[33] Grape-seed extracts contain rich flavonoids, mainly oligomeric procyanidins (OPC), which have been widely used as cross-linking agents, chemical anticancer agents, or antibacterial agents.[34]

In this contribution, we report a simple and fast approach to fabricate injectable, self-healing, adhesive, and antibacterial hydrogels based on CMCS and OPC. Water-soluble CMCS is nontoxic, biodegradable, antibacterial, and antifungal. OPC rich in polyphenols serves as a "crosslinking agent" to crosslink CMCS into a hydrogel network. By controlling the concentration of OPC, the properties of resulting hydrogels could be well controlled. Additionally, the combination of CMCS and OPC provides a rapid and universal method for the design of antibacterial hydrogel dressings.

School of Life Science, Zhengzhou University, 100 Science Road, Zhengzhou 450001, P. R. China. E-mail: yao453343550@126.com; guanfangxia@126.com

2.   Materials and methods

2.1   Materials

Carboxymethyl chitosan (CMCS, degree of carboxylation ≥ 80%) was purchased from Yuanye Bio-Technology Co., Ltd. (Shanghai, China). The original chitosan used for preparation of CMCS is sourced from shrimp shells and the degree of deacetylation is ≥75%. Oligomeric procyanidins (OPC, 60–85% purity) from grape seeds were obtained from Tianjin Jianfeng Natural Product R&D Co., Ltd. All bacteria used in this study were purchased from Beina Biology Co., Ltd. (Beijing, China).

2.2   Preparation of CMCS/OPC hydrogels

For the preparation of CMCS/OPC hydrogels, precursor solutions A and B were separately prepared by dissolving CMCS and OPC in water at desired concentrations and mixed subsequently. Specifically, CMCS was dissolved in water to achieve a concentration of 60 mg mL^{-1} (precursor solution A). Precursor solution B was prepared by dissolving OPC in water to achieve a concentration of 40, 80, and 120 mg mL^{-1}. Hydrogels with CMCS final concentration of 30 mg mL^{-1} (3%) and OPC final concentration of 20 mg mL^{-1} (2%), 40 mg mL^{-1} (4%), or 60 mg mL^{-1} (6%) were prepared by mixing equal volume of precursor solution A and B. For convenience, the hydrogels containing 2%, 4%, and 6% OPC were named CMCS/OPC$_2$, CMCS/OPC$_4$, and CMCS/OPC$_6$, respectively. For all CMCS/OPC hydrogels, the concentration of CMCS was maintained at 3%.

2.3   FTIR analysis of CMCS/OPC hydrogels

To investigate the gelatinization mechanism of hydrogels, 400 mg CMCS powder, 400 mg OPC powder and 400 mg lyophilized CMCS/OPC$_4$ hydrogel were prepared, and the spectra of samples were recorded by Fourier transform infrared spectroscopy (Nicolet-6700, Thermal Sciences, USA). Spectra were recorded in the range of 400–4000 cm^{-1}.

2.4   Characterization of CMCS/OPC hydrogels

2.4.1   Rheological characterization of hydrogels. The storage modulus (G') and loss modulus (G'') of the CMCS/OPC hydrogels were measured by employing a TA rheometer (DHR-2) at 37 °C. The constant strain was set at 1% with a fixed frequency of 1.0 Hz.

2.4.2   SEM of hydrogels. The internal structure of CMCS/OPC hydrogels were characterized by scanning electron microscopy (SEM, FEI Quanta200, Netherlands) after vacuum freeze-drying, crushing, and gold-spraying.

2.4.3   Swelling behavior of hydrogels. Briefly, different groups of hydrogels with similar size and shape were immersed into the PBS at 37 °C and taken out at a regulated time interval. Blot the surface of hydrogels with a filter paper and weigh it. Use the following formula to calculate the swelling ratio of hydrogel:

$$\text{Swelling ratio} = [(w_t - w_0)/w_0] \times 100\%,$$

where w_t represented the weight of hydrogel after swelling and w_0 meant the weight of hydrogel before swelling.

2.5   Injectable and self-healing tests

The injectable ability of hydrogel was tested. First, CMCS/OPC$_4$ hydrogel was loaded into a syringe with a 25 G needle, then injected into a transparent glass bottle with water and drew letters in a Petri dish. Afterward, hydrogels were subjected to shear thinning tests: the viscosity change of the hydrogel was detected at 25 °C under the shear rate range of 1–100 s^{-1}.

The self-healing capability of hydrogel was measured by visual and qualitative methods. Firstly, the self-healing behavior was observed macroscopically. Specifically, cut the hydrogel in half along the diameter, bring the two halves together and incubate for 1 min, then the healed hydrogel was suspended under gravity. For the qualitative test, the hydrogel was prepared as a disk with a 20 mm in diameter and a 1 mm in height. Using the strain amplitude sweep method (γ changed from 1% to 1000%, 1 Hz), the value of the critical strain region was detected. Then a new hydrogel with the same size was used to test the self-healing behavior. Amplitude oscillatory strains were switched from small strain ($\gamma = 1.0\%$, 60 s for each interval) to large strain ($\gamma = 500\%$, 20 s for each interval), and 5 cycles were carried out in the test.

2.6   Adhesive test

The adhesive capability of hydrogel was estimated by visual and quantitative methods. To put it simply, a group of 200 μL CMCS/OPC$_4$ hydrogels were prepared to test the adhesiveness to abiotic tissues (wood, iron, plastic, glass, rubber) and biological tissues (heart, liver, spleen, lung, kidney) respectively.

The adhesive strength of hydrogels was quantitatively measured by pig skin lap shear test. First, fresh pig skin bought from a local supermarket (YONGHUI SUPERSTORES) was soaked in normal saline to remove the fat layer, and then cut into 50 mm × 25 mm rectangular pieces. The CMCS/OPC$_4$ hydrogel was injected between two pig skin samples, and the size of hydrogel was 25 mm × 10 mm. After bonding, the lap shear test was carried out on an electronic universal testing machine (CMT2102, MTS) in a tensile mode at a tensile rate of 5 mm min^{-1}. Finally, the maximum tensile strength was recorded.

2.7   Antibacterial test

The inherent antibacterial property of CMCS/OPC hydrogels was verified by the surface antibacterial activity test and inhibition zone test.[35,36] The details of surface antibacterial activity test were as following. First, 100 μL CMCS/OPC hydrogels were prepared in 24 well-plate using sterilized CMCS and OPC solutions in a sterile environment, then 10 μL bacteria solution containing 10^7 CFU mL^{-1} *Escherichia coli* or *Staphylococcus aureus* was added to the surface of hydrogel. After co-culture for 2 h, 1 mL sterile medium was added to each well for re-suspension, from which 100 μL suspension was moved to a new well and followed by adding 1 mL fresh medium and further culture for 18–24 h. The absorbance of suspension at 600 nm and the number of viable bacteria were measured with a microplate analyzer. The results were expressed as lethal percentage:
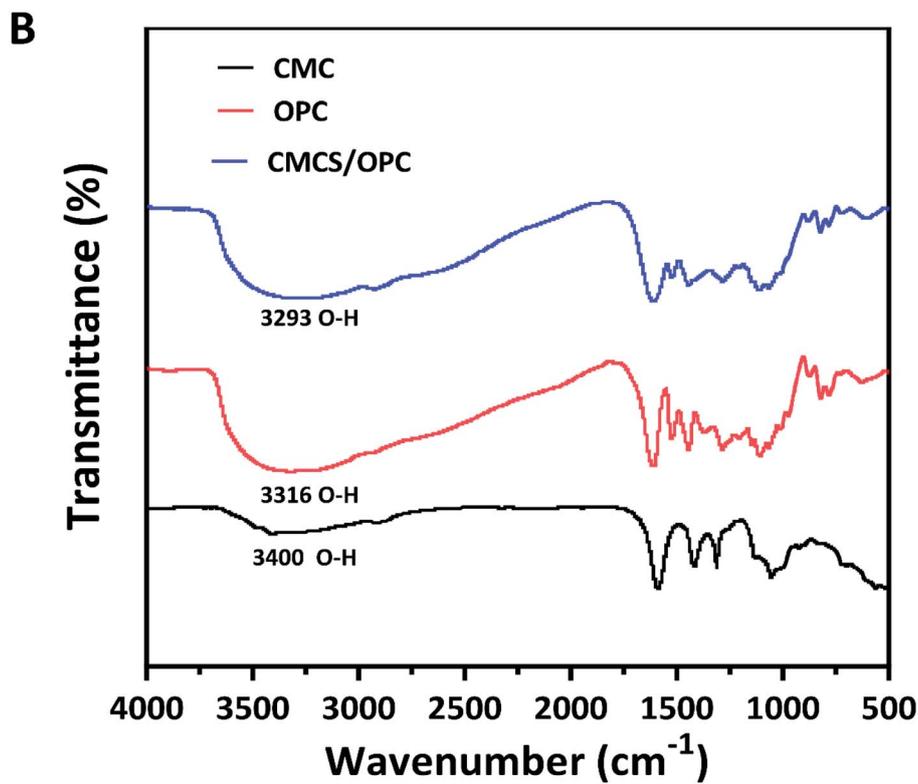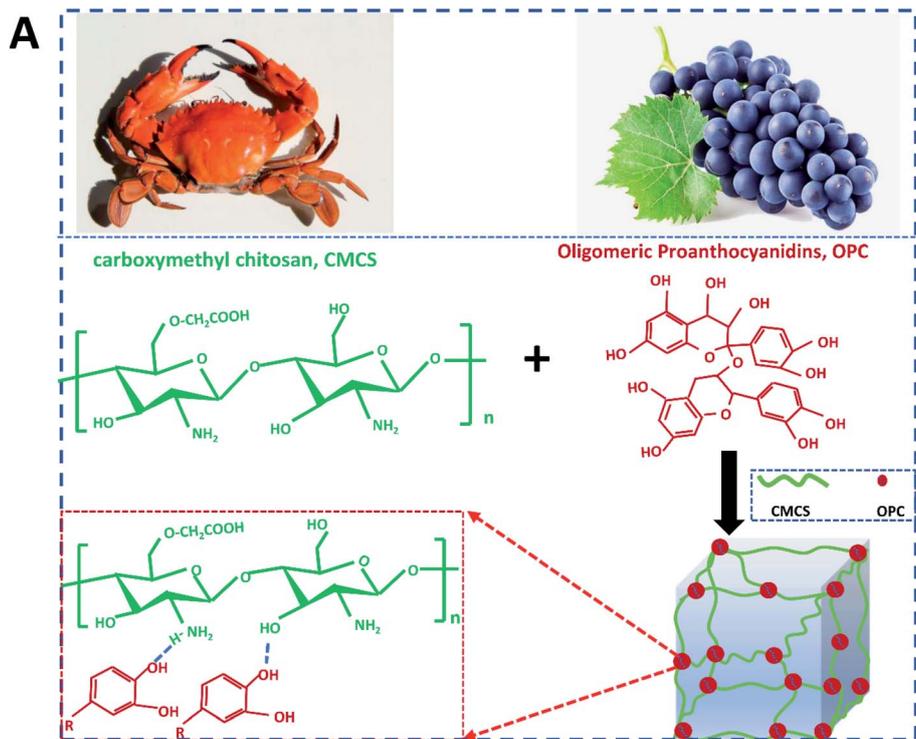
Fig. 1   (A) Schematical formation of CMCS/OPC hydrogel and the interaction between CMCS and OPC; (B) FTIR spectra of CMCS powder, OPC powder, and lyophilized CMCS/OPC$_4$ hydrogel.

Bacterial killing ratio (%) = $(A_{control} - A_{hydrogel})/A_{control} \times 100\%$

where $A_{control}$ is the absorbance of control group without hydrogel, $A_{hydrogel}$ is the absorbance of hydrogel group.

For the bacteriostatic zone experiment, 100 μL bacterial suspension (10^7 CFU mL^{-1}) were seeded on the surface of agar plate. The hydrogels, 3% CMCS solution and 4% OPC solution were then brought into full contact with bacteria on the solid medium. After incubation at 37 °C for 16–24 h, photos were taken and the diameter of inhibition circle was measured.

3. Results and discussion

3.1 Preparation and FTIR analysis of CMCS/OPC hydrogels

In this study, a simple one-step method was implemented to prepare multifunctional hydrogels based on CMCS from natural crab and OPC from natural grape, and these hydrogels were named CMCS/OPC. CMCS/OPC hydrogels were quickly formed under physiological condition when CMCS and OPC solutions were simply blended. In this hydrogel system, OPC acts as the crosslinker, and its polyphenol groups could form dynamic hydrogen bonds with hydroxy (–OH), carboxyl (–COOH), and amino (–NH$_2$) groups on CMCS branch chain (Fig. 1A).

To determine the driving force of hydrogel self-assembly, the FTIR spectra of OPC powder, CMCS powder, and lyophilized CMCS/OPC$_4$ hydrogel were performed and shown in Fig. 1B. According to previous reports, the characteristic peaks at 3400 cm^{-1} and 3316 cm^{-1} were considered to the –OH stretching vibration of CMCS and OPC, respectively.[33,37] After CMCS and OPC formed hydrogel, the absorption band of –OH stretching vibration moved to 3293 cm^{-1}, confirming the existence of hydrogen bond interaction during the gelation process.[30,38,39] To analyze the influence of OPC on the properties of hydrogel, CMCS/OPC hydrogels with three different OPC content were fabricated. For the convenience of description, hydrogel containing 2, 4, or 6 wt% OPC was abbreviated as CMCS/OPC$_2$, CMCS/OPC$_4$, and CMCS/OPC$_6$, respectively.

3.2 Characterization of CMCS/OPC hydrogels

3.2.1 Gelation time of CMCS/OPC hydrogels.
Herein, the gelation time of CMCS/OPC hydrogels was measured by an inverted test tube method. According to Fig. 2A, the gelation time was 125.3 s for CMCS/OPC$_2$ hydrogel, 18.7 s for CMCS/OPC$_4$ hydrogel, and only 5.3 s CMCS/OPC$_6$ hydrogel. Clearly, the gel speed accelerated with the growing of OPC content. More OPC means more polyphenol groups in hydrogel network, which strengthens the formation of hydrogen bonds between polyphenol groups and hydroxy/carboxyl/amino groups, finally accelerates the gelation process.[40]

3.2.2 Rheological characterization of CMCS/OPC hydrogels.
The viscoelastic behavior of hydrogels was studied by rheological test, and the storage modulus is usually used as an indicator of the stiffness of a given viscoelastic material. In this study, the linear viscoelastic behavior of hydrogels was characterized by scanning measurement of oscillation frequency, and the results were presented in Fig. 2B. At an angular frequency of 100 rad s^{-1}, the storage modulus (G') of CMCS/OPC$_2$, CMCS/OPC$_4$, and CMCS/OPC$_6$ hydrogels were 27 Pa, 42 Pa, and 64 Pa, respectively. The cross-linking degree of CMCS/OPC hydrogels increased with growing of OPC concentration, thereby the mechanical property of hydrogels was enhanced.[34,41,42]

3.2.3 Swelling behavior, degradation and SEM of CMCS/OPC hydrogels.
Water uptake by the hydrogels was characterized *via* their swelling ratio. As shown in Fig. 2C, swelling ratio of CMCS/OPC hydrogels in PBS gradually increased and then reached their maximum swelling ratio within 3 h at 37 °C, then quickly degraded. This swelling-then-erosion behavior without
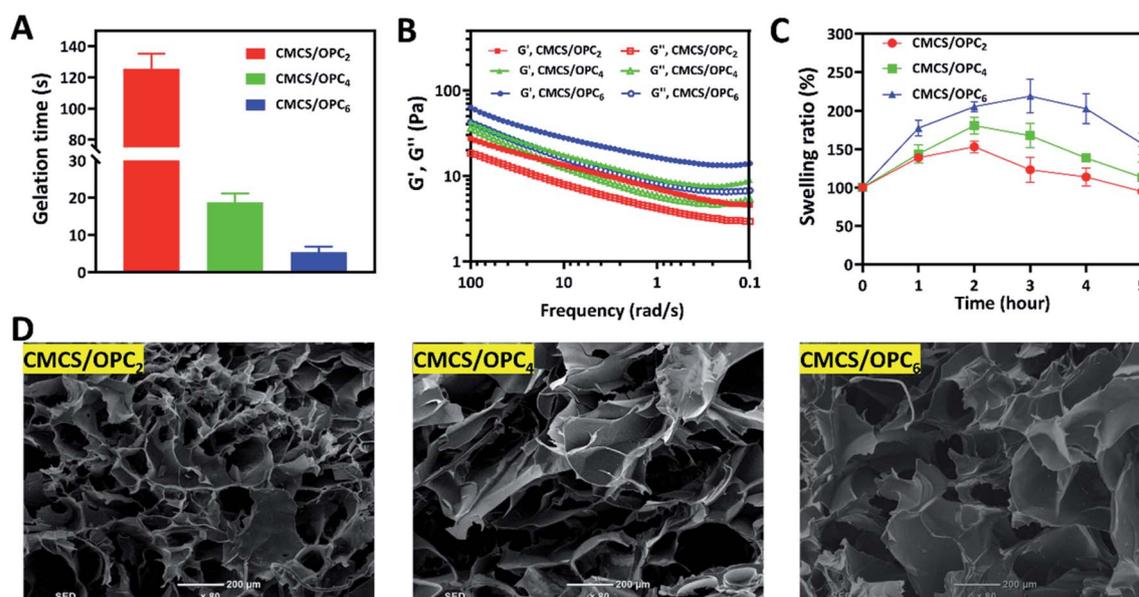

Fig. 2 (A) Gelation time of CMCS/OPC hydrogels; (B) storage modulus (G') and loss modulus (G'') of CMCS/OPC hydrogels *versus* frequency; (C) swelling ratio of the CMCS/OPC hydrogels in PBS; (D) SEM images of freeze-dried CMCS/OPC hydrogels, scale bar is 200 μm.

swelling equilibrium, suggesting that the resulted hydrogel is mainly a physically-crosslinked hydrogel. The swelling ratio of CMCS/OPC$_2$ hydrogel was 153.1%, CMCS/OPC$_4$ hydrogel was 180.6%, and CMCS/OPC$_6$ hydrogel increased to 219.1%. This may be due to the increase of OPC concentration, which increases the degree of cross-linking in the hydrogel and eventually leads to the increase of swelling ratio.[43] In addition, the degradation of hydrogels was studied. From the result in Fig. S1,† CMCS/OPC hydrogels could be completely degraded within 11 days *in vitro*.
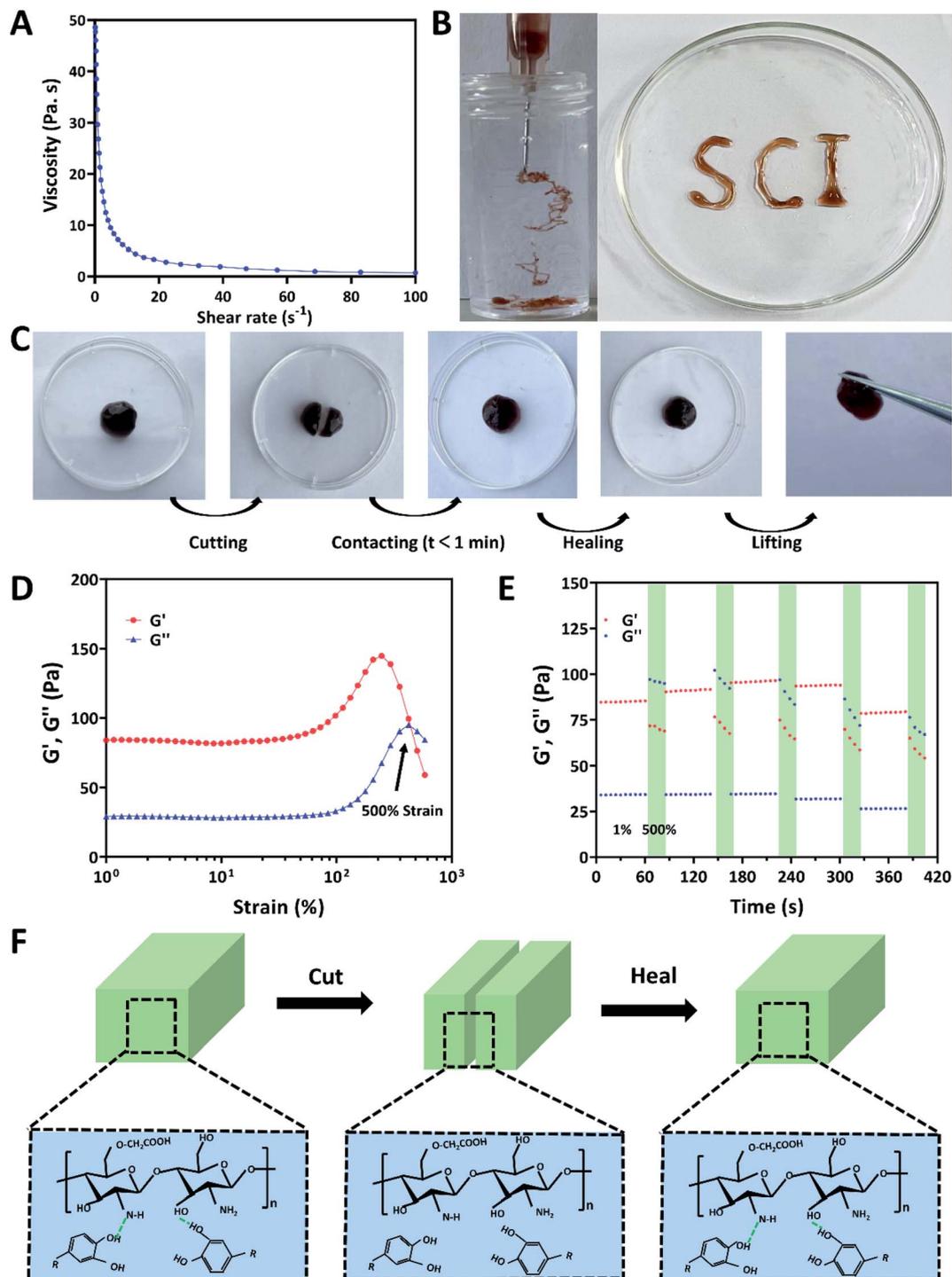

Fig. 3 (A) Shear-thinning test of CMCS/OPC$_4$ hydrogel; (B) photographs of injectable of CMCS/OPC$_4$ hydrogel; (C) photographs of self-healing process of CMCS/OPC$_4$ hydrogel; (D) G' and G'' on strain sweep and the rheological properties of CMCS/OPC hydrogels when alternate step strain switched from 1% to 1000%; (E) self-healing property of CMCS/OPC$_4$ hydrogel and the rheological property of the hydrogel when alternate step strain switched from 1% to 500%; (F) illustration presents the self-healing property of hydrogel.

The internal morphology of freeze-dried CMCS/OPC hydrogels was observed by SEM and displayed in Fig. 2D. All hydrogels exhibited well-defined 3D pore structures with inherent interconnectivity which met the design requirement of mimicking native ECM.[34,44] Increasing OPC content leaded to larger pore size of freeze-dried CMCS/OPC hydrogels, which was agreed with the swelling phenomenon.

3.3 Injectable and self-healing properties of CMCS/OPC hydrogels

Injectable hydrogels have attracted widespread attention due to their painless and minimally invasive features. Hydrogels with shear dilution ability can be injected directly into the desired injury site, filling the site well and making full contact with the desired site, avoiding the existence of gaps. Therefore, the relationship between viscosity and shear rate of hydrogels was studied by rheometer. As presented in Fig. 3A, with the shear rate increased, the viscosity of CMCS/OPC$_4$ hydrogel continued

to decrease, indicating this hydrogel has good shear-thinning property. This shear-thinning behavior can be attributed to the shear-induced breaking of dynamic hydrogel network that enhances the injectability of hydrogel. *In vitro* injectable test was shown in Fig. 3B, CMCS/OPC$_4$ hydrogel could be easily injected and maintained its shape after injection without breaking, clogging, or dissolving, formed "SCI" shaped letters.

Common hydrogels tend to crack or rupture when exposed to external tension or tissue activity. The destruction of hydrogel will not only cause the deterioration or even loss of its own performance, but also cause the invasion of external bacteria.[45] Therefore, it is important to ensure the structural integrity of hydrogel dressings. The self-healing property of CMCS/OPC$_4$ hydrogel were detected by both visible and qualitative methods without adding any additive. Results of the visible method were shown in Fig. 3C. Firstly, the hydrogel was injected into a dish to obtain a complete hydrogel block. Then, when CMCS/OPC$_4$ hydrogel was cut into two pieces and followed by placing
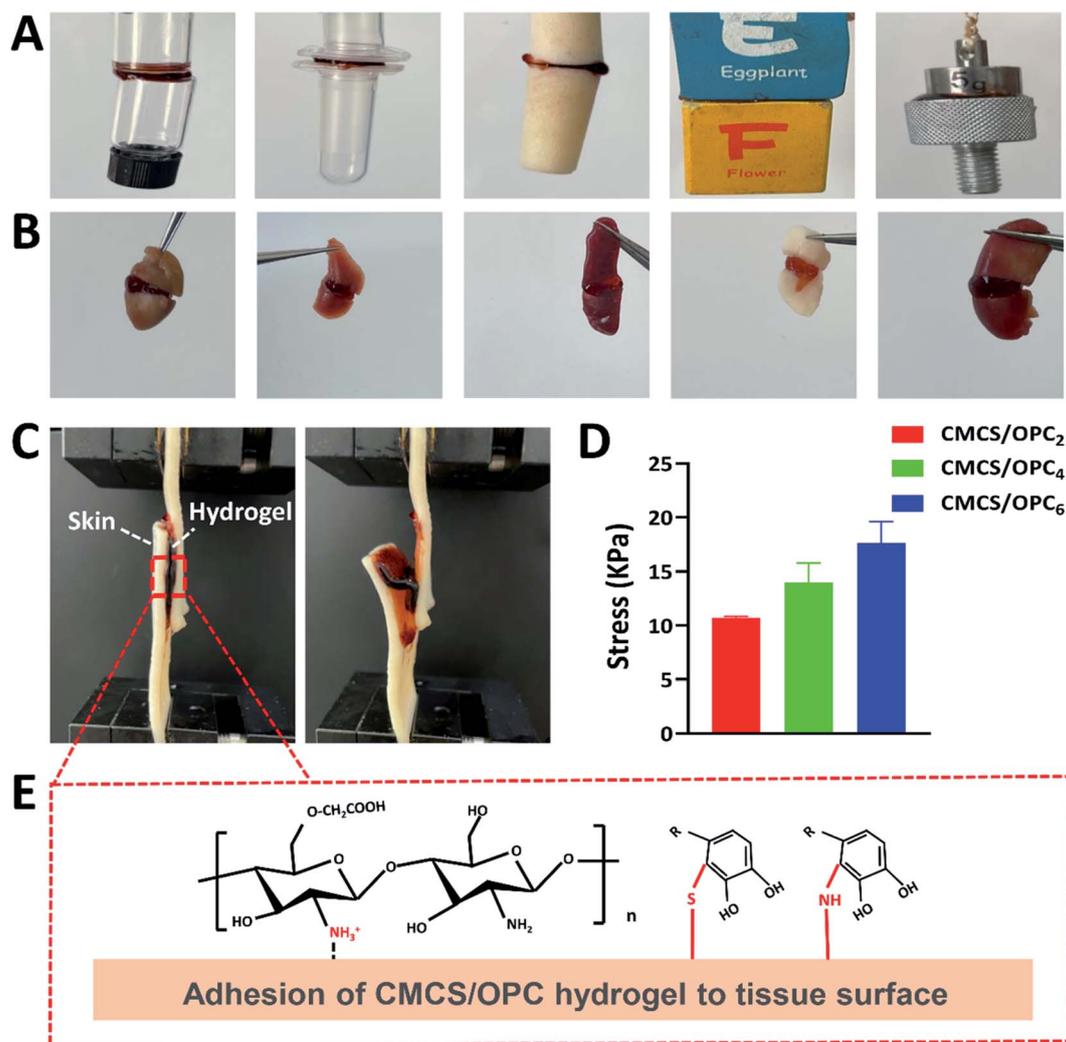

Fig. 4 (A) Adhesive exhibition of CMCS/OPC hydrogels adhering to diverse materials, including glass, wood, plastic, rubber, iron; (B) exhibition of CMCS/OPC hydrogels adhering to biological tissues including heart, liver, spleen, lung, kidney; (C) schematic presentation of the lap shear test; (D) adhesive strength of hydrogels; (E) illustration presents the hydrogel's adhesive property. Data are reported as means ± SD.

together. After contacting for 1 min without external force, the cut hydrogel was healed and showed no cracks, and it could bear its own weight. The self-healing ability of CMCS/OPC$_4$ hydrogel was further qualitatively evaluated by a rheological recovery test. The strain scanning result of hydrogel was shown in Fig. 3D. When the strain was 500%, G' intersects with G'', which is the critical point of collapse of hydrogel network. When the strain exceeds the critical strain, G' drops sharply. Subsequently, continuous strain scans were performed to determine the self-healing behavior of hydrogel (Fig. 3E). When 500% high dynamic strain was applied, G' value drops from ∼85 Pa to ∼34 Pa, lower than G'', indicating hydrogel network collapse. When a lower concentration of 1% strain was applied, the values of G' and G'' were almost restored to their original values even after five alternating cycles. Which demonstrates the excellent autonomous healing capability of CMCS/OPC hydrogel. These results confirm that the designed CMCS/OPC hydrogel has good self-healing ability. We attributed its excellent self-healing performance to the dynamic hydrogen bonds

in CMCS/OPC hydrogel networks. The self-healing mechanism of CMCS/OPC hydrogel was shown in Fig. 3F.

3.4 Adhesion of CMCS/OPC hydrogels

As shown in Fig. 4A, CMCS/OPC hydrogel can adhere to various materials, including glass, wood, plastic, rubber, and iron. In addition, CMCS/OPC hydrogel has special tissue adhesion, as shown in Fig. 4B, CMCS/OPC hydrogel can easily adhere to different biological tissues such as heart, liver, spleen, lung, kidney, and skin. Furthermore, the adhesive performance of CMCS/OPC hydrogels were quantitatively characterized through lap shear test with porcine skin as a model of biological tissue (Fig. 4C and D). The adhesion strength of CMCS/OPC$_2$, CMCS/OPC$_4$, and CMCS/OPC$_6$ hydrogels was 10.7 kPa, 14 kPa, and 17.7 kPa, respectively. The tight adhesion between CMCS/OPC hydrogels and the skin surface was attributed to covalent and hydrogen bond interactions. As shown in Fig. 4E, –CONH and –OH groups in the porcine skin surface could interact with –OH
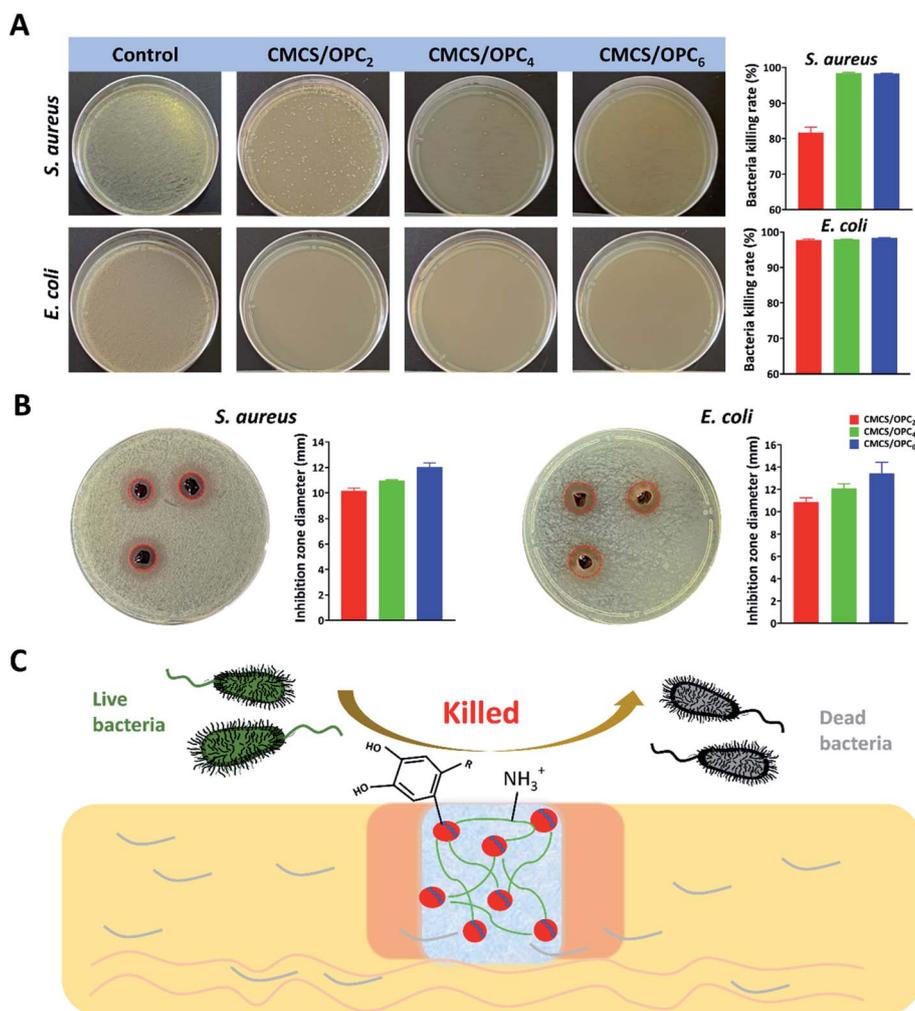

Fig. 5 (A) Photographs and quantitative statistics of bacterial killing ratio of CMCS/OPC hydrogels against *S. aureus* and *E. coli* in the antibacterial performance test; (B) photographs and quantitative statistics of inhibition zone against *S. aureus* and *E. coli* in the zone of inhibition test; (C) schematic illustration of antibacterial capability involving the bacterial destruction induced by the polyphenol groups and protonated amino groups of hydrogels. Data are reported as means ± SD.

and polyphenol groups in hydrogel surface *via* hydrogen bonding. The incorporation of OPC can improve the adhesive ability of hydrogel.[11,46,47]

3.5 Antibacterial property of CMCS/OPC hydrogels

Gram-positive *Staphylococcus aureus* (*S. aureus*) and Gram-negative *Escherichia coli* (*E. coli*) are two common pathogenic bacteria. So, we evaluated the antibacterial performance of CMCS/OPC hydrogels against *S. aureus* and *E. coli* by two methods. Firstly, the antibacterial ability of hydrogels was verified by direct contact. As shown in Fig. 5A, after contacting with hydrogels for 2 h at 37 °C, the inhibition ratios against *S. aureus* in CMC/OPC₄ hydrogel and CMC/OPC₆ hydrogel groups were more than 95%, while the inhibition ratio of CMC/OPC₂ hydrogel against *S. aureus* was only 81.7%. For *E. coli*, the antibacterial ratios of all tested hydrogels were more than 95%.

In addition, the bacteriostasis of CMCS/OPC hydrogels, 3% CMCS solution and 4% OPC solution was further evaluated by a bacteriostatic zone test. The results were shown in Fig. 5B. After 24 hours of contacting with hydrogels, all groups had a significant inhibition zone. The diameters of antibacterial zone in CMCS/OPC₂, CMCS/OPC₄ and CMCS/OPC₆ hydrogel groups against *S. aureus* were 10.2, 11.0, 12.0 mm and that against *E. coli* were 10.9, 12.06, 13.4 mm, respectively. The range of antibacterial zone increased with increase of OPC concentration, which may be caused by the diffusion of OPC. The antibacterial ability of 3% CMCS solution and 4% OPC solution were also investigated and results were presented in Fig. S2.† Both CMCS and OPC possessed good antibacterial capability, while the effect of OPC was obviously better than CMCS. These above findings confirm that CMCS/OPC hydrogels have good antibacterial activity. The potentially mechanism of antibacterial capability involves the bacterial destruction induced by the polyphenol groups and protonated amino groups form CMCS/OPC hydrogels (Fig. 5C).[2,48,49]

4. Conclusions

In conclusion, we have developed a simple one-step method for the preparation of oligomeric procyanidin-crosslinked carboxymethyl chitosan hydrogels (CMCS/OPC). The dynamically intermolecular hydrogen bonds are responsible for gel formation, which endow hydrogel with fast gelation speed, flexible injectability, self-healing and adhesive capabilities. In addition, CMCS/OPC hydrogels have broad-spectrum antibacterial ability. In view of these excellent properties, the prepared hydrogels have great potential as antibacterial materials.

Author contributions

Yuanmeng He: resources, writing – original draft, preparation. Shen Guo: resources, methodology, writing – review & editing. Rong Chang: methodology. Dan Zhang: writing – review & editing. Yikun Ren: writing – review & editing. Fangxia Guan: conceptualization, writing – review & editing. Minghao Yao: conceptualization, validation, investigation, writing – review & editing.

Conflicts of interest

The authors declare no competing financial interest.

References

1 E. M. Ahmed, *J. Adv. Res.*, 2015, **6**, 105–121.
2 Y. Liang, J. He and B. Guo, *ACS Nano*, 2021, **15**, 12687–12722.
3 Z. Li, B. Li, X. Li, Z. Lin, L. Chen, H. Chen, Y. Jin, T. Zhang, H. Xia, Y. Lu and Y. Zhang, *Carbohydr. Polym.*, 2021, **267**, 118155.
4 X. Zhang, D. Yao, W. Zhao, R. Zhang, B. Yu, G. Ma, Y. Li, D. Hao and F.-J. Xu, *Adv. Funct. Mater.*, 2021, **31**, 2009258.
5 E. Lee and B. Kim, *Korean J. Chem. Eng.*, 2011, **28**, 1347.
6 Z. Q. Lei, H. P. Xiang, Y. J. Yuan, M. Z. Rong and M. Q. Zhang, *Chem. Mater.*, 2014, **26**, 2038–2046.
7 A. K. Blakney, A. B. Little, Y. Jiang and K. A. Woodrow, *Drug Delivery*, 2017, **24**, 582–590.
8 M. Monavarian, S. Kader, S. Moeinzadeh and E. Jabbari, *Tissue Eng., Part B*, 2019, **25**, 294–311.
9 J. Xu, Z. Fan, L. Duan and G. Gao, *Polym. Chem.*, 2018, **9**, 2617–2624.
10 J. Radhakrishnan, A. Subramanian, U. M. Krishnan and S. Sethuraman, *Biomacromolecules*, 2017, **18**, 1–26.
11 X. Du, Y. Liu, X. Wang, H. Yan, L. Wang, L. Qu, D. Kong, M. Qiao and L. Wang, *Mater. Sci. Eng., C*, 2019, **104**, 109930.
12 B. Zhang, J. He, M. Shi, Y. Liang and B. Guo, *Chem. Eng. J.*, 2020, **400**, 125994.
13 W. Wang, R. Narain and H. Zeng, *Front. Chem.*, 2018, **6**, 497.
14 D. L. Taylor and M. in het Panhuis, *Adv. Mater.*, 2016, **28**, 9060–9093.
15 S. Guo, M. Yao, D. Zhang, Y. He, R. Chang, Y. Ren and F. Guan, *Adv. Healthc. Mater.*, 2022, **11**, 2101808.
16 K. Shatalin, A. Nuthanakanti, A. Kaushik, D. Shishov, A. Peselis, I. Shamovsky, B. Pani, M. Lechpammer, N. Vasilyev, E. Shatalina, D. Rebatchouk, A. Mironov, P. Fedichev, A. Serganov and E. Nudler, *Science*, 2021, **372**, 1169–1175.
17 K. Chen, C. Tong, J. Yang, P. Cong, Y. Liu, X. Shi, X. Liu, J. Zhang, R. Zou, K. Xiao, Y. Ni, L. Xu, M. Hou, H. Jin and Y. Liu, *J. Mater. Sci. Technol.*, 2021, **63**, 236–245.
18 L. Xia, S. Wang, Z. Jiang, J. Chi, S. Yu, H. Li, Y. Zhang, L. Li, C. Zhou, W. Liu and B. Han, *Carbohydr. Polym.*, 2021, **264**, 117965.
19 S. Yang, X. Li, P. Liu, M. Zhang, C. Wang and B. Zhang, *ACS Biomater. Sci. Eng.*, 2020, **6**, 4666–4676.
20 D. R. Perinelli, L. Fagioli, R. Campana, J. K. W. Lam, W. Baffone, G. F. Palmieri, L. Casettari and G. Bonacucina, *Eur. J. Pharm. Sci.*, 2018, **117**, 8–20.
21 S. Chen, M. Liu, S. Jin and Y. Chen, *Polym. Bull.*, 2014, **71**, 719–734.

22 L. Weng, N. Rostambeigi, N. D. Zantek, P. Rostamzadeh, M. Bravo, J. Carey and J. Golzarian, *Acta Biomater.*, 2013, **9**, 8182–8191.

23 M. C. G. Pellá, M. K. Lima-Tenório, E. T. Tenório-Neto, M. R. Guilherme, E. C. Muniz and A. F. Rubira, *Carbohydr. Polym.*, 2018, **196**, 233–245.

24 P. Luo, M. Nie, H. Wen, W. Xu, L. Fan and Q. Cao, *Int. J. Biol. Macromol.*, 2018, **113**, 1024–1031.

25 Z. Shariatinia and A. M. Jalali, *Int. J. Biol. Macromol.*, 2018, **115**, 194–220.

26 Q.-Z. Zhong, S. Li, J. Chen, K. Xie, S. Pan, J. J. Richardson and F. Caruso, *Angew. Chem., Int. Ed.*, 2019, **58**, 12563–12568.

27 L. Zhang, S.-S. Wan, C.-X. Li, L. Xu, H. Cheng and X.-Z. Zhang, *Nano Lett.*, 2018, **18**, 7609–7618.

28 H. Montazerian, A. Baidya, R. Haghniaz, E. Davoodi, S. Ahadian, N. Annabi, A. Khademhosseini and P. S. Weiss, *ACS Appl. Mater. Interfaces*, 2021, **13**, 40290–40301.

29 C. Wang, H. Zhou, H. Niu, X. Ma, Y. Yuan, H. Hong and C. Liu, *Biomater. Sci.*, 2018, **6**, 3318–3331.

30 N. Li, X. Yang, W. Liu, G. Xi, M. Wang, B. Liang, Z. Ma, Y. Feng, H. Chen and C. Shi, *Macromol. Biosci.*, 2018, **18**, 1800209.

31 Y. Yang, Y. Liang, J. Chen, X. Duan and B. Guo, *Bioact. Mater.*, 2022, **8**, 341–354.

32 X. Zhang, G.-h. Sun, M.-p. Tian, Y.-n. Wang, C.-c. Qu, X.-j. Cheng, C. Feng and X.-g. Chen, *Int. J. Biol. Macromol.*, 2019, **138**, 321–333.

33 Y. Liang, X. Zhao, Y. Hu, Y. Han and B. Guo, *J. Colloid Interface Sci.*, 2019, **556**, 514–528.

34 H. Ma, Q. Zhou, J. Chang and C. Wu, *ACS Nano*, 2019, **13**, 4302–4311.

35 H. Liu, C. Wang, C. Li, Y. Qin, Z. Wang, F. Yang, Z. Li and J. Wang, *RSC Adv.*, 2018, **8**, 7533–7549.

36 S. Guo, M. Yao, D. Zhang, Y. He, R. Chang, Y. Ren and F. Guan, *Adv. Healthc. Mater.*, 2021, 2101808.

37 W. Huang, Y. Wang, Y. Chen, Y. Zhao, Q. Zhang, X. Zheng, L. Chen and L. Zhang, *Adv. Healthc. Mater.*, 2016, **5**, 2813–2822.

38 M. Shin, K. Kim, W. Shim, J. W. Yang and H. Lee, *ACS Biomater. Sci. Eng.*, 2016, **2**, 687–696.

39 X. Yu, L. Wang, B. Xu, P. Wang, M. Zhou, Y. Yu and J. Yuan, *Eur. Polym. J.*, 2021, **150**, 110411.

40 H. Lei and D. Fan, *Chem. Eng. J.*, 2021, **421**, 129578.

41 J. Yu, X. Chen, Y. Yang, X. Zhao, X. Chen, T. Jing, Y. Zhou, J. Xu, Y. Zhang and Y. Cheng, *J. Mater. Chem. B*, 2020, **8**, 3058–3063.

42 Y. J. Wang, X. N. Zhang, Y. Song, Y. Zhao, L. Chen, F. Su, L. Li, Z. L. Wu and Q. Zheng, *Chem. Mater.*, 2019, **31**, 1430–1440.

43 L. Teng, Z. Shao, Q. Bai, X. Zhang, Y.-S. He, J. Lu, D. Zou, C. Feng and C.-M. Dong, *Adv. Funct. Mater.*, 2021, **31**, 2105628.

44 M. Farokhi, F. Mottaghitalab, Y. Fatahi, A. Khademhosseini and D. L. Kaplan, *Trends Biotechnol.*, 2018, **36**, 907–922.

45 B. Chen, Y. Liang, L. Bai, M. Xu, J. Zhang, B. Guo and Z. Yin, *Chem. Eng. J.*, 2020, **396**, 125335.

46 J. Qu, X. Zhao, Y. Liang, T. Zhang, P. X. Ma and B. Guo, *Biomaterials*, 2018, **183**, 185–199.

47 Y. Li, X. Wang, Y.-n. Fu, Y. Wei, L. Zhao and L. Tao, *ACS Appl. Mater. Interfaces*, 2018, **10**, 26046–26055.

48 I. Younes and M. Rinaudo, *Mar. Drugs*, 2015, **13**, 1133–1174.

49 T. Wang, X.-K. Zhu, X.-T. Xue and D.-Y. Wu, *Carbohydr. Polym.*, 2012, **88**, 75–83.